Desalination and Water Treatment
www.deswater.com

doi: 10.5004/dwt.2017.21560

95 (2017) 234–246
November

Adsorption of Ni^{2+}, Hg^{2+}, Pb^{2+}, Cr^{3+}, and Co^{2+} on iron oxide nanoparticles immobilized on cellulose fiber: equilibrium, kinetic, thermodynamic, mechanisms, and statistical supposition

Attarad Ali[a], Sania Naz[a], Abdul Mannan[b], Muhammad Fahad Shams[c], Ijaz Hussain[d], Muhammad Zia[a,*]

[a]*Department of Biotechnology, Quaid-i-Azam University, Islamabad 45320, Pakistan, Tel. +92-51-9064-4126; emails: ziachaudhary@gmail.com (M. Zia), attarad.ali@kiu.edu.pk (A. Ali), sanianaz0@gmail.com (S. Naz)*
[b]*Department of Pharmaceutical Sciences, COMSATS Institute of Information Technology, Abbottabad, Pakistan, email: abdulmannan_ka@yahoo.com*
[c]*Preston Institute of Nanosciences and Technology, Islamabad, Pakistan, email: fahad.shams4928956@gmail.com*
[d]*Department of Statistics, Quaid-i-Azam University, Islamabad 45320, Pakistan, email: ijaz@qau.edu.pk*

Received 4 April 2017; Accepted 16 October 2017

ABSTRACT

Metallic nanoparticles (NPs) are of immense significance due to supra properties especially for contaminant remediation from water. However, NPs release in ecosystem is also threatening. To overcome this prospect, iron oxide (Fe_2O_3) NPs were composited with cellulose fibers (FeCt) by simple co-precipitation method, and used for removal of mercury, chromium, cobalt, lead, and nickel ions from synthetic wastewater. The batch experiments determined that adsorption kinetics follow Langmuir isotherm model and best fit in pseudo-second-order reaction. FeCt composite material exhibited enhanced metal adsorption capacity as compared with cellulose polymer. The competitive capacity of all five heavy metals onto the adsorbents followed the adsorption order as $Ni^{2+} > Hg^{2+} > Pb^{2+} > Cr^{3+} > Co^{2+}$ that is also related to the nature and strength of electrostatic interaction among metal ions. The statistical inference (Hotelling's t^2 statistics and t test) supports adsorption kinetics. The synthesized NPs composite material can be efficiently used for treatment of wastewater in domestic and industrial water filtration plants.

Keywords: Cellulose; Iron oxide nanoparticles; Wastewater; Adsorption; Heavy metal

1. Introduction

Wastewater management is one of the main environmental issue since the toxins particularly heavy metals gain access to surface water and groundwater which may be used for drinking purpose [1,2]. Accumulation of metal ions may lead to serious ecological and health problems that are unanimously recognized as carcinogenic and non-biodegradable inorganic pollutants [3]. Therefore, elimination of toxic heavy metals from wastewater has become crucial to protect human population and the environment. Some heavy metals are predominantly important in cleaning from wastewaters such as arsenic, mercury, chromium, cadmium, lead, and nickel [4,5]. Several methods such as coagulation–flocculation, chemical precipitation, flotation, electrolytic reduction, ion-exchange and membrane technologies, exist for the removal of harmful metal ions [6]. Currently, adsorption is an alternative treatment procedure. Natural and low-cost adsorbent materials, that is, industrial by-products, agricultural waste, zeolites, clays and chemically modified polymeric materials have been studied for adsorption of heavy metals [2].

Various solid-phase sorbents (e.g., ion imprinted polymers, carbon nanotubes, nanoparticles [NPs], fullerenes, and biosorbents) have been examined to treat wastewater. These innovative materials are considered superior to the

* Corresponding author.

traditional agents having upgraded performance in the withdrawal of target analytes [7]. However, these methods have some drawbacks, that is, maintenance or operation costs, high capital, slow speed or limited capacity, and laborious procedures [8]. Hence, there should be simple, comparatively fast, quantitative, and economical collection processes. One of the ultimate requirements of any adsorbent or metal collector is its capacity to be renewed and recycled over a number of adsorption/desorption cycles [9].

Cellulose fibers have been used in several applications as biosorbent by reason of their advantages and properties such as high adsorption capacity and poor electrical conductivity. Cellulose derivatives have been used in water treatment for both organic and inorganic contaminants [10–14] due to the intrinsic properties such as renewability, biocompatibility, favorable hydrophilicity, and biodegradability [15–18]. The commercially available cotton fiber is a kind of renewable and recyclable cellulose that is appropriate for fabricating novel type of functional materials [19,20]. The most contemporary known method of modification is the impregnation or coating of NPs onto the porous surface of cellulose fibers [21]. In comparison, magnetic adsorbent is also considered as an effective and rapid technique for separating cations from aqueous solutions because of better separation ability and less energy requirement [22]. Iron oxide NPs have been extensively researched in the separation technologies because of its cost-effective preparation, simple surface modification or coating and the ability to manipulate or control materials on a nanoscale dimensions, which exhibit excellent versatility in the field of separation and environmental techniques [23–31]. However, release of NP in treated water itself pollutes the treated water. To overcome this problem, binding the NP with polymers support is ultimate solution.

The aim of this study was to investigate five different toxic metal ions (Hg^{2+}, Cr^{3+}, Co^{2+}, Pb^{2+}, and Ni^{2+}) adsorption at normal conditions on cotton impregnated with Fe_2O_3 NPs (FeCt). We examined the synthesis and structure of the fabricated FeCt material using Fourier transform infrared spectroscopy (FTIR), X-ray powder diffraction (XRD), and scanning electron microscopy (SEM). The adsorption equilibrium of toxic metal ions on the FeCt is also investigated through isotherms and pseudo-order reaction kinetics followed by statistical validation.

2. Materials and methods

All the reagents used were of analytical grade. Double distilled water was used throughout. Laboratory glassware was kept overnight in 10% (v/v) HNO_3 solution and then rinsed with double distilled water. The nitrate salts of Hg^{2+}, Cr^{3+}, Co^{2+}, Ni^{2+}, and Pb^{2+} of analytical grade (Merck, Germany) were used without further purification. Cotton wool (commercial grade), ferrous sulfate heptahydrate ($FeSO_4.7H_2O$), ferric chloride hexahydrate ($FeCl_3.6H_2O$), urea, ammonium hydroxide (NH_4OH) and ethanol were purchased from Aldrich (USA).

2.1. Synthesis of Fe_2O_3 NPs impregnated cotton (FeCt)

The commercially available bulk cotton cluster was slashed into small pieces before use and thoroughly washed with water and absolute ethanol. Thereafter, the cellulose was sonicated for 15–20 min (three times) in ice cold water and dried overnight in oven at 50°C.

The sample (FeCt adsorbent) was prepared by modifying the method applied in our previous study [32,33] collectively with the technique used by Jiang et al. [34] for particles synthesis.

Stoichiometric ratio 1:2 of ferrous sulfate heptahydrate ($FeSO_4.7H_2O$) and ferric chloride hexahydrate ($FeCl_3.6H_2O$) was dissolved in deionized water under vigorous stirring to prepare 0.2 M ferrite solution as an iron source. Concentrated ammonia was diluted in an aqueous solution to form 3.5 M ammonium hydroxide (NH_4OH) as a base source. Finally, 1 g dried cotton wool (cellulose) was first immersed in 500 mL of ferrite solution and then 10 g of urea was also added. The mixture was heated gently up to 80°C–100°C on constant stirring at 250 rpm for 1 h to decompose urea. Thereafter, during rigorous stirring, the mixture was titrated to have a pH of around 10–11 by adding drops of 3.5 M ammonium hydroxide at room temperature. It was observed that the color of material and solution became brown owing to the formation of Fe_2O_3 particles. The brown mixture was then heated again at 60°C–70°C in a water bath for 30 min yielding Fe(III)-loaded cotton (FeCt). The material was thoroughly washed with deionized water.

2.2. Characterization

2.2.1. Fourier transform infrared spectroscopy

FTIR analysis of the prepared sample material (FeCt) was performed to elucidate the role of different functional moieties while deposition of Fe_2O_3 on cotton surface. For this purpose bench-top Spectrum™ 65 was used having a 4,000–600 cm^{-1} frequency ranges with 16 scans per spectrum of speed.

2.2.2. X-ray diffraction (crystallographic structure)

Successful deposition of Fe_2O_3 NPs on cotton (FeCt) and crystallinity was studied by XRD analysis using X'Pert³ Powder (PANalytical, Netherlands) with nickel monochromate having theta ranges from 20° to 80°. Wavelength of radiation source (Cu Kα) was 1.5406 Å. A voltage of 40 kV with 30 mA of current at room temperature is the working conditions of XRD. Using Scherrer's equation ($D = 0.9\lambda/\beta\cos\theta$) crystalline size of as prepared NPs was calculated, where D is the average size, λ is the X-ray's wavelength (1.5406 Å), β corresponds to angular full width at half maximum, and θ is the diffraction angle.

2.2.3. Scanning electron microscopy

Morphological studies of Ct and FeCt were carried out using JEOL-JSM-6490LA SEM (JEOL, Tokyo, Japan). Operating conditions of SEM were supply of 20 kV voltage with a 2,838 cps counting rate. Micrographs produced by SEM analysis give idea about the deposition of Fe_2O_3 NPs on cotton.

2.3. Preparation of heavy metal stock solution

The stock solutions of mercury, chromium, cobalt, lead, and nickel were prepared in deionized water from standard

heavy metal solutions. The pH of the stock solutions was adjusted to 5.5 using 0.1% NaOH or HCl.

2.4. Batch adsorption experiments

The adsorption experiments were carried out in batch mode. A 1,000 mL of an artificial wastewater sample by adding different concentrations (2–8 mg/L) of metal salts was treated with 0.5 and 1 g of both FeCt and Ct (control) at optimum pH (5.5) and 25°C. The mixture in conical flask was shaken at 150 rpm for 400 min and the concentration of five metal ions (Hg(II), Cr(III), Co(II), Pb(II), and Ni(II)) was analyzed after every 10 min using atomic absorption spectrometer on flame mode (model PerkinElmer AAS 800).

The adsorption capacities at any time (q_t, mg/g) and at equilibrium (q_e, mg/g) were calculated using the following equations:

$$q_t = (C_0 - C_t)V/m \quad (1)$$

$$q_e = (C_0 - C_e)V/m \quad (2)$$

where C_0 is the initial concentration of metal ions (mg/L), C_t is the concentration of metal ions at any time t (mg/L), C_e is the concentration of metal ions at equilibrium (mg/L), V is the volume of the metal ions solution (L), and the m is the weight of adsorbent used (g).

The removal ratio (R%) at adsorption equilibrium was calculated using the following equation:

$$R = (C_0 - C_e)/C_0 \times 100\% \quad (3)$$

3. Results and discussion

Cotton functionalized by Fe_2O_3 NPs has been successfully synthesized and characterized. The synthesized composite materials efficiently removed metal ions from water under ambient conditions.

3.1. Characterization of Ct and FeCt nanocomposite

3.1.1. FTIR analysis

FTIR pattern of cotton and FeCt samples presented that Fe_2O_3 is successfully linked on the surface of cotton. All those peaks that appear in cotton intensified in FeCt nanocomposite depicting that a strong bonding exist between cotton and Fe_2O_3 NPs. FTIR pattern of pure cotton obtained at 3,402, 2,926, and 1,749–1,579 cm^{-1} is due to O–H, C–H, and C–O stretching, respectively, while incidence of peaks at 1,491–1,109 and 1,058–945 cm^{-1} arise due to functional moieties of ester and carboxyl groups [19,35]. Majority of peaks raised at 615–845 cm^{-1} attribute to C–H bending vibrations (Fig. 1). On the other hand, intense peaks in case of FeCt nanocomposite observed from 3,402 up to 1,300 cm^{-1} show that strong bonding occurs between Fe_2O_3 NPs and cellulose due to hydroxyl group (–OH) [36]. Majority of peaks that appeared at a range of 1,300–615 cm^{-1} disappeared and characteristics peaks at 875, 689, and 637 cm^{-1} indicate the presence of iron oxide particles [37].

3.1.2. XRD analysis

Major diffraction peaks observed for both Ct and FeCt nanocomposite corresponds to the angle of 22.92°, 41.99°, 48.92°, and 72.51° in Ct while 23.10°, 35.99°, 42.08°, 43.61°, 48.69°, 49.54°, and 72.01° in FeCt (Fig. 2). Diffraction peaks observed at 35.99°, 43.61°, and 49.54° indexing (110), (400), and (024) are characteristic peaks for Fe_2O_3 while other peaks are same as observed for Ct. These results show that Fe_2O_3 was successfully coated on the surface of cotton. Our results are consistent with other studies [38,39].

3.1.3. SEM analysis

In order to study the morphological changes on the surface of Ct upon treating with Fe_2O_3, SEM was performed (Fig. 3). In case of pure Ct, fiber-like morphology is observed that is covered by Fe_2O_3 in case of FeCt nanocomposite verifying successful coating of Fe_2O_3 on the surface of cotton.

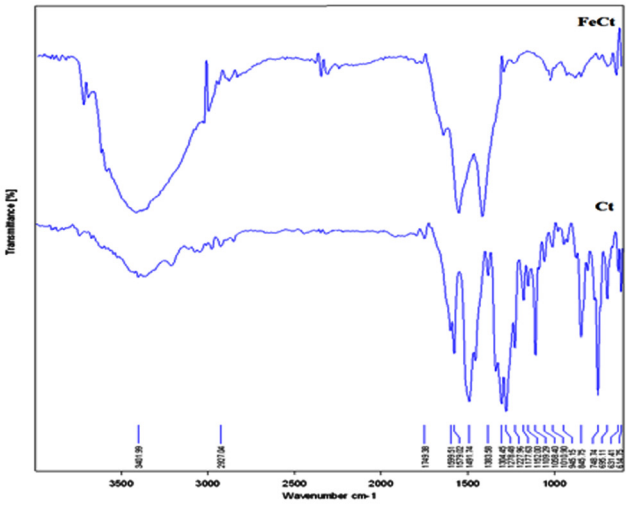

Fig. 1. FTIR of cotton (Ct) and iron nanoparticles impregnated cotton (FeCt).

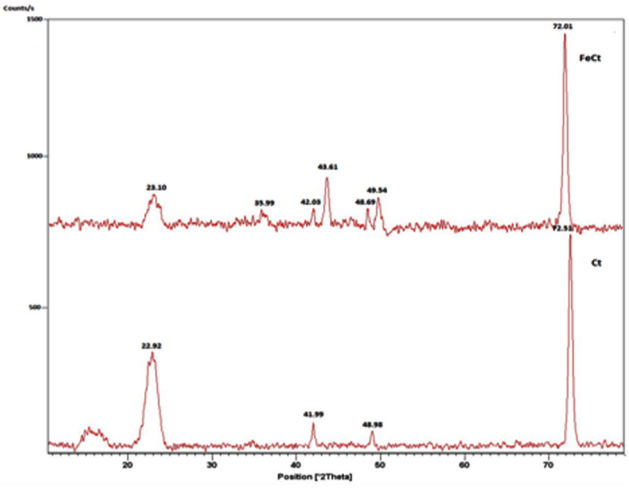

Fig. 2. X-ray diffraction patterns of Ct and FeCt nanocomposites.

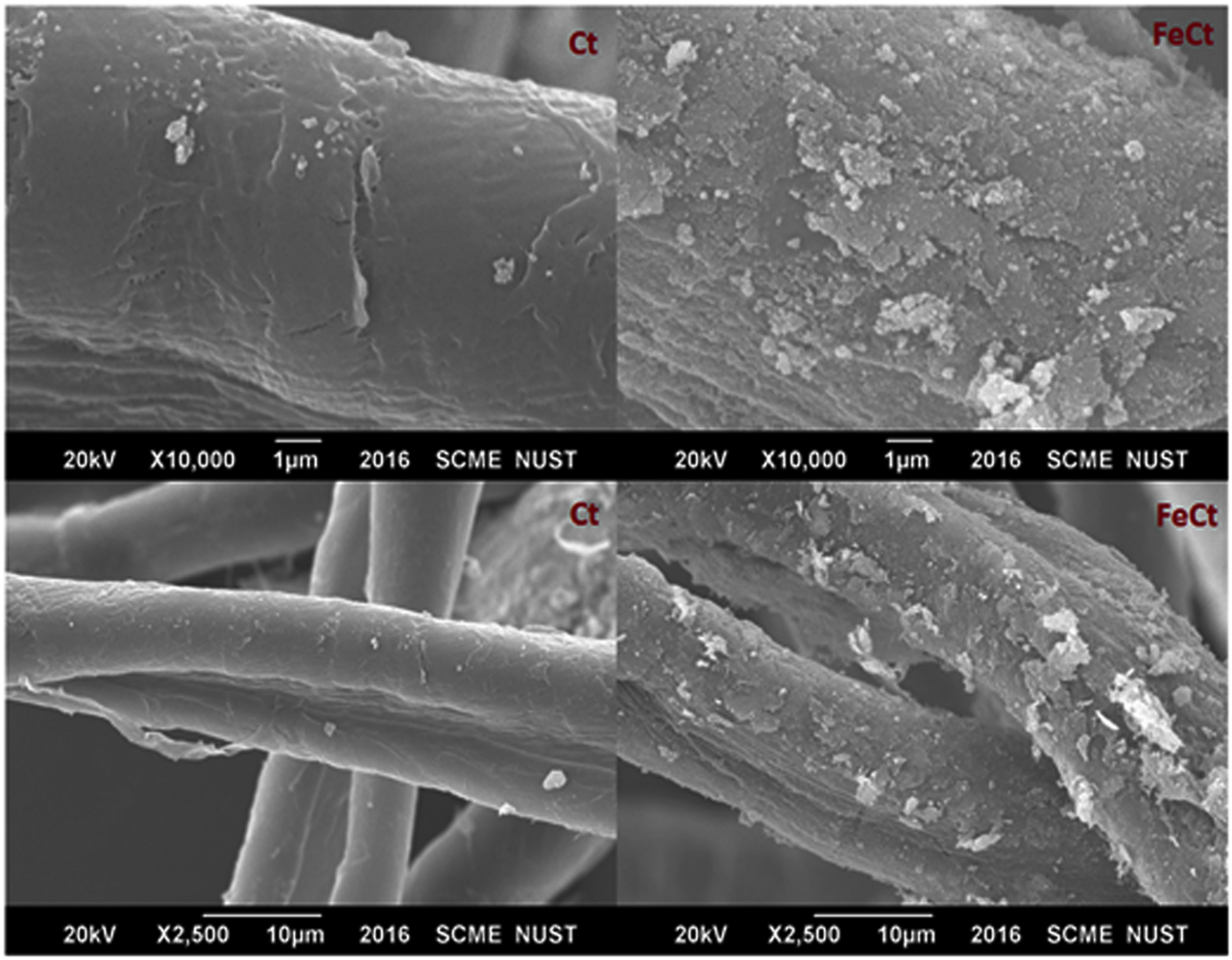

Fig. 3. SEM images of Ct and FeCt nanocomposites.

SEM analysis also shows that size of Fe_2O_3 was in the range of nanoscale.

3.2. Solution pH and concentration of metal ions

Two concentrations of adsorbent (0.5 and 1 g) were treated with heavy metals concentrations from 2 to 8 ppm at pH 5.5 and room temperature. Figs. 4(A)–(D) describe that the percentage removal of Cr^{3+} is almost 99% and 90% for FeCt concentrations 0.5 and 1 g, respectively, but the control (Ct) did not show better removal percentage (55%–70%). The percentage removal order achieved is in the sequence of $Cr^{3+} > Hg^{2+} > Ni^{2+} > Pb^{2+} > Co^{2+}$. Lead and cobalt showed very lesser removal percentage (5%–15%) with control; however, more than 50% removal percentage was achieved with the sample FeCt (Fig. 4). The adsorption efficiency is higher in case of 0.5 g FeCt for all metal ions removal except Co^{2+} ion. The maximum uptake was achieved within 30–50 min whereafter, it became constant. This means that the studied cellulose-based adsorbent (FeCt) has fast kinetics relative to solitary cellulose fibers with different functionalities [40]. This might also be attributed to the hydrophilic as well as swelling character of cellulose. The initial rapid rate of adsorption might be due to the availability of the vacant active surfaces of the adsorbents for cationic species in the solution. Later slow adsorption rate is due to the electrostatic hindrance caused by already adsorbed adsorbates and slow pore diffusion of the ions [41].

3.3. Kinetics studies on heavy metal adsorption

The batch adsorption kinetics of Hg^{2+}, Cr^{3+}, Co^{2+}, Pb^{2+}, and Ni^{2+} by Ct and FeCt is assessed with three models: pseudo-first-order kinetic, pseudo-second-order kinetic, and intra-particle diffusion models, to decipher the controlling mechanism of the adsorption process. The pseudo-first-order model is expressed as [11,14,42]:

$$\log(q_e - q_t) = \log q_e - K_1 t/2.303 \quad (4)$$

where K_1 is the rate constant of pseudo-first-order (min^{-1}). The kinetic parameters were determined from the linear plot of (t/q_t) vs. t for pseudo-second-order or of $\log(q_e - q_t)$ vs. t for pseudo-first-order. The validity of each model was checked

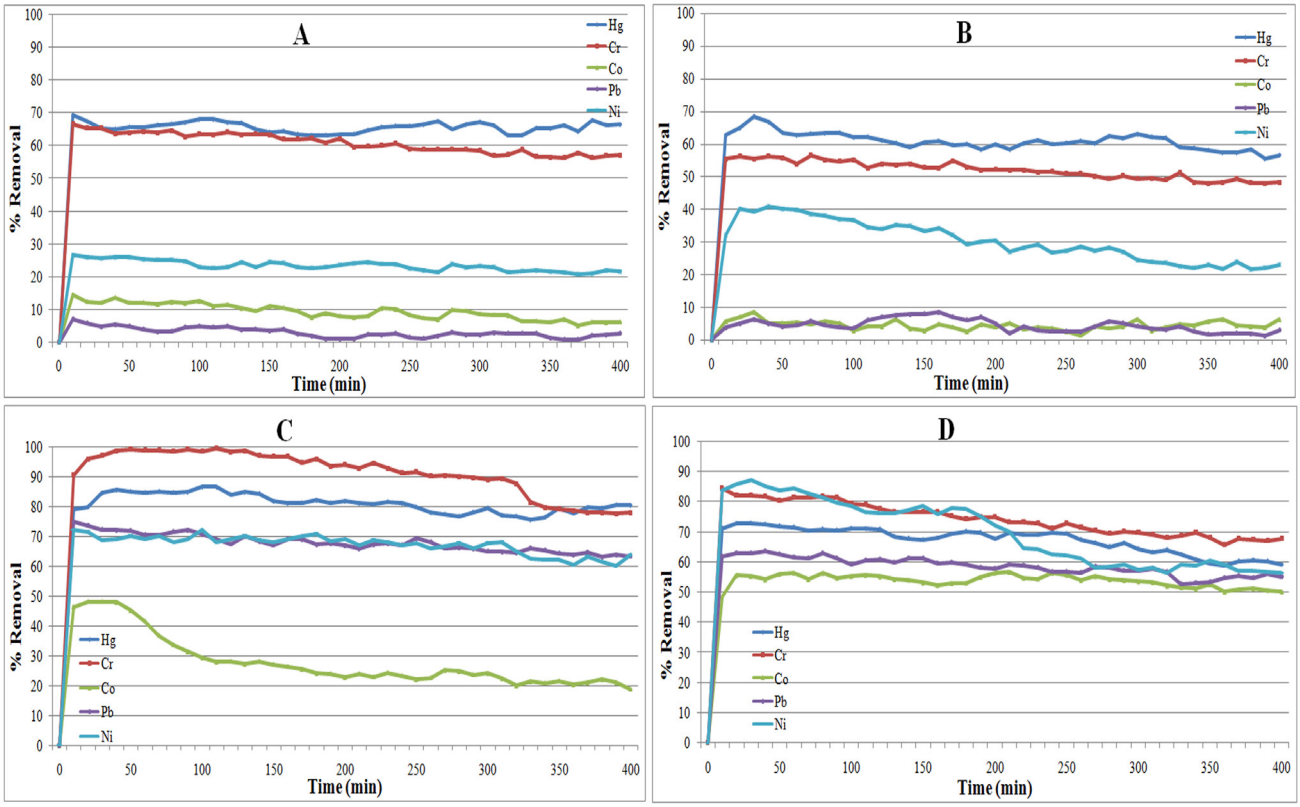

Fig. 4. Effect of contact time on the metal ions removal by cotton cellulose (A) 0.5 g, (B) 1 g as control (Ct) and Fe_2O_3 impregnated cotton cellulose (FeCt) shown as (C) 0.5 g and (D) 1 g.

by the fitness of the straight line (R^2) as well as the consistence between experimental and calculated values of q_e. The data were found to fit well the pseudo-second-order model as shown in Fig. 5 and Tables 1 and 2.

The pseudo-second-order model is expressed as [24–26,43]:

$$t/q_t = 1/K_2 q_e^{\,2} + 1t/q_e \quad (5)$$

where K_2 is the pseudo-second-order rate constant of adsorption (g/mmol min), q_e and q_t (mmol/g) refer the amount of metal ion adsorbed at equilibrium and at time (t), respectively.

Fig. 5 displays the pseudo-second-order kinetic of Hg^{2+}, Cr^{3+}, Co^{2+}, Pb^{2+}, and Ni^{2+} onto Ct and FeCt at two different concentrations. As presented in Tables 1 and 2, parameters (R^2) of pseudo-second-order kinetic model ($R^2 > 0.9$) are bigger than those of both the other two models for all the concentrations. Furthermore, q_e experimental values agree well with the calculated q_e values by using the pseudo-second-order model.

The transferring of Hg^{2+}, Cr^{3+}, Co^{2+}, Pb^{2+}, and Ni^{2+} from water to the surface of Ct and FeCt samples comprises several steps (e.g., adsorption on the pore surface, external diffusion, surface diffusion, and pore diffusion) [44]. During the process of the adsorption at the outside surface of the samples (Ct and FeCt), heavy metals may move from the surface of fibers to the inner pores through intra-particle diffusion, which is generally a relatively slow process. Hence, the intra-particle diffusion model was estimated with the following equation [45]:

$$q = K_i t^{1/2} + c \quad (6)$$

where K_i is the rate constant of the intra-particle diffusion (mg/g $min^{1/2}$) and c is the intercept. If a straight line passing through the origin in this model is presented from plotting a graph of q_t vs. $t^{1/2}$, it is possible that the process of adsorption is comprised of diffusion of heavy metals. The rate constant of intra-particle transport (K_i) is obtained by the slope of the linear curve.

The rate of adsorption is possibly affected by various factors including the concentration of the adsorbate, the degree of mixing, the size of the adsorbate molecule and its affinity to the adsorbents, the size distribution of the adsorbent, the diffusion coefficient of the adsorbate in the bulk phase, and so on. The results reveals that although the process of adsorption of Hg^{2+}, Cr^{3+}, Co^{2+}, Pb^{2+}, and Ni^{2+} onto the FeCt cannot be simulated by the model of the intra-particle diffusion very well, the pore diffusion still include in the process of adsorption because of the porous nature of FeCt.

3.4. Equilibrium studies on heavy metals adsorption

Langmuir and Freundlich isotherm models were selected to evaluate the adsorption process. Contact time of 50 min

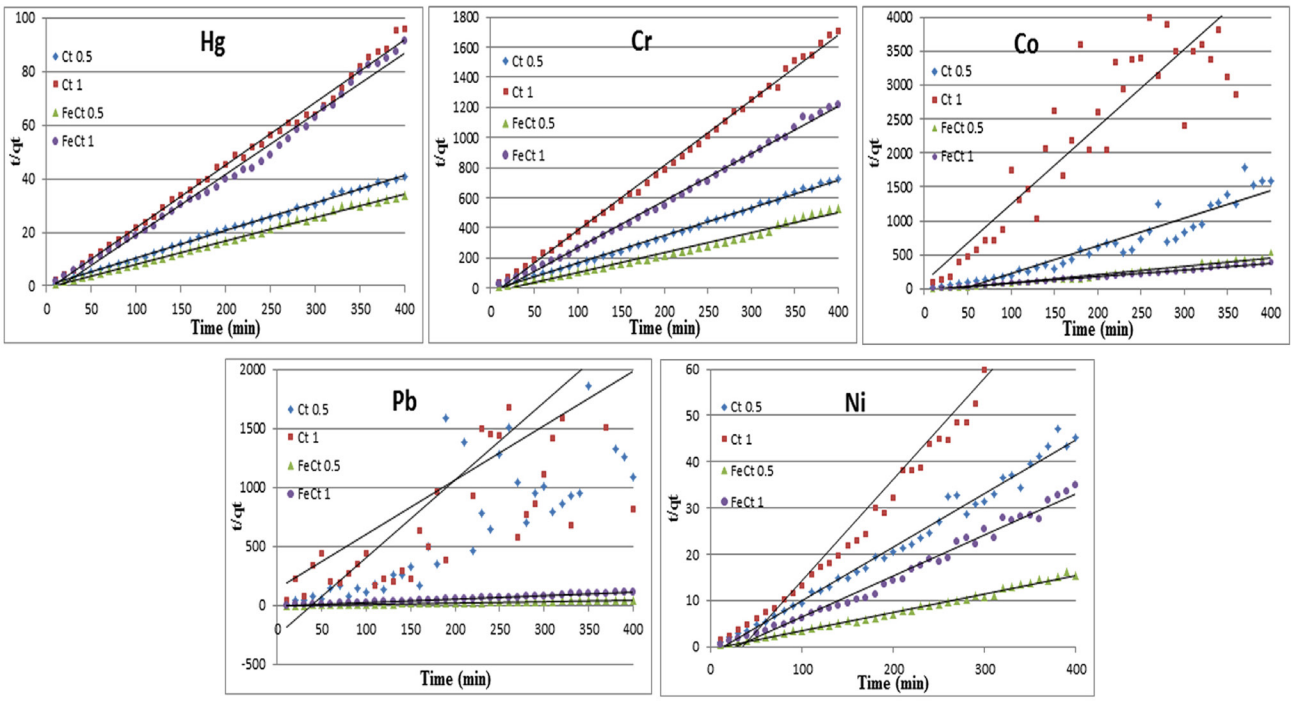

Fig. 5. Pseudo-second-order kinetic adsorption model plots for the adsorption of Hg^{2+}, Cr^{3+}, Co^{2+}, Pb^{2+}, and Ni^{2+} ions by two concentrations (0.5 and 1 g) of adsorbents (Ct and FeCt).

Table 1
Pseudo-second-order and pseudo-first-order adsorption parameters of Hg^{2+}, Ni^{2+}, Cr^{3+}, Co^{2+}, Pb^{2+}, and Ni^{2+} ions for control cotton

Metals	Pseudo-second-order reaction kinetics					Pseudo-first-order reaction kinetics		
	q_e (exp)	q_e (cal)	k	h	R^2	$-k$	log(q_e)	R^2
For 0.5 g control (Ct)								
Hg	10.30	9.710	0.380	9.710	0.998	0.0011	–0.3657	0.053
Cr	0.646	0.543	0.160	0.049	0.998	0.0034	–1.5807	0.998
Co	0.586	0.243	0.091	0.005	0.907	0.0034	–1.0225	0.371
Pb	1.034	0.177	5.031	0.159	0.070	0.0027	–0.5121	0.274
Ni	11.30	8.330	0.008	0.613	0.986	0.0039	–0.1849	0.493
For 1 g control (Ct)								
Hg	5.050	4.275	0.033	0.604	0.995	0.0018	–0.438	0.303
Cr	0.274	0.231	0.001	0.019	0.997	0.0055	–2.225	0.337
Co	0.170	0.059	0.721	0.002	0.590	0.0004	–1.049	0.006
Pb	0.652	0.184	0.295	0.010	0.460	0.0011	–0.602	0.022
Ni	8.890	4.545	0.0064	0.133	0.966	0.0043	–0.014	0.755

was considered as equilibrium time of the adsorption process of Hg^{2+}, Cr^{3+}, Co^{2+}, Pb^{2+}, and Ni^{2+} onto FeCt.

3.4.1. Langmuir adsorption isotherm

The Langmuir adsorption isotherm predicts the maximum monolayer adsorption capacity of FeCt and determines whether the adsorptive process is favorable for this model or not. Fig. 6 presents the plots of C_e/q_e vs. C_e for the Langmuir adsorption isotherms of Hg^{2+}, Cr^{3+}, Co^{2+}, Pb^{2+}, and Ni^{2+} removal onto Ct and FeCt at 0.5 and 1 g. The correlation coefficients (R^2) and constant parameters are summarized in Table 3. The linearized Langmuir isotherms are as follows:

$$C_e/q_e = (C_e/Q_m) + 1/(bQ_m) \quad (7)$$

where b represents the Langmuir adsorption constant (L/mg), C_e represents the solute concentration at equilibrium (mg/L),

Table 2
Pseudo-second-order and pseudo-first-order adsorption parameters of Hg^{2+}, Ni^{2+}, Cr^{3+}, Co^{2+}, Pb^{2+}, and Ni^{2+} ions by iron nanoparticles impregnated cotton

Metals	Pseudo-second-order reaction kinetics					Pseudo-first-order reaction kinetics		
	q_e (exp)	q_e (cal)	k	h	R^2	$-k$	log(q_e)	R^2
For 0.5 g FeCt								
Hg	12.79	11.47	0.013	1.804	0.997	0.0036	–0.480	0.451
Cr	0.940	0.757	0.062	0.035	0.986	–0.0025	–0.652	0.035
Co	1.950	0.809	0.039	0.026	0.970	0.00368	–0.473	0.230
Pb	9.684	8.163	0.013	0.917	0.998	0.00345	–0.359	0.481
Ni	30.26	25.12	0.003	2.163	0.992	0.00299	0.1386	0.268
For 1 g FeCt								
Hg	5.390	4.348	0.014	0.267	0.991	0.0073	–1.209	0.581
Cr	0.410	0.319	2.067	0.021	0.997	0.0039	–1.682	0.304
Co	1.142	1.031	0.121	0.128	0.996	0.0027	–1.505	0.066
Pb	4.123	3.521	0.028	0.349	0.997	0.0048	–0.990	0.575
Ni	17.80	11.36	0.003	0.420	0.985	0.0062	–0.119	0.781

Q_m represents the maximum concentration retained by the adsorbent (mg/g), and q_e represents the adsorption capacity in equilibrium (mg/g). The maximum adsorption amounts calculated are 71.43, 22.73, 0.77, 24.16, and 69.45 mg/g for Hg^{2+}, Cr^{3+}, Co^{2+}, Pb^{2+}, and Ni^{2+} onto 0.5 g FeCt, respectively, whereas the maximum adsorption amounts calculated for 1 g FeCt are 11.81, 1.75, 1.31, 6.11, and 75.76 mg/g for Hg^{2+}, Cr^{3+}, Co^{2+}, Pb^{2+}, and Ni^{2+}, respectively. Similarly, the maximum adsorption amounts for all metal ions were also calculated for the control material (Ct) at 0.5 and 1 g (Table 3). The competitive capacity of all five heavy metals onto the adsorbents follow the adsorption order as $Ni^{2+} > Hg^{2+} > Pb^{2+} > Cr^{3+} > Co^{2+}$. This is related to the nature and strength of interaction. The observed higher value for Ni^{2+} and Hg^{2+} might be attributed to the higher electrostatic interaction. The higher value for other cations also attributes to the strength of bond formation (stability) along with Jahn–Teller effect which is predominant for such cationic complexes like that of Cu^{2+} [27,28,30,31,46].

3.4.2. Freundlich isotherm model

The Freundlich isotherm model is based on multilayer adsorption process and the equation is as follows:

$$\log q_e = \log k + (1/n)\log C_e \quad (8)$$

where k and n represent isotherm constant of this model that suggest the intensity and capacity of adsorption, respectively. In this model, the constants k and n correlate with adsorption mechanism and the rate of adsorption of heavy metals. The parameters and correlation coefficients of Freundlich model are listed in Table 4. The values of k and n change with the conditions applied such as increase or decrease in adsorbent and adsorbate concentrations as well as temperature [22,31], and commonly the value of n remains bigger than 1, suggesting that Hg^{2+}, Cr^{3+}, Co^{2+}, Pb^{2+}, and Ni^{2+} favorably adsorbed by FeCt on both concentrations. In addition, the higher value of n suggests the formation of stronger bond between heavy metal ions and FeCt adsorbents.

The R^2 value for Ct and FeCt of Langmuir and Freundlich isotherm is greater than 0.9. However, for both concentrations of FeCt, the Langmuir isotherm values of constants and R^2 (>0.99) from Tables 3 and 4 show more perfection when compared with Freundlich isotherm. Hence, the best fitted isotherm for FeCt is Langmuir isotherm which specifies the occurrence of adsorption process on the homogenously monolayered surface of the sorbent [30,32,47].

3.5. Desorption of heavy metals and reuses

The iron-oxide NPs respond very well to magnetic fields without any permanent magnetization so the FeCt samples can be easily separated with a magnet. This characteristic is very vital for the industrial and water treatment applications.

3.6. Design of the cotton fibers and mechanism of adsorption

In view of all the above results, the schematic illustration of the preparation of FeCt and the mechanism of adsorption of heavy metal ions onto FeCt is proposed and illustrated in Fig. 7. In this work, it is attempted to design a novel cellulose-based adsorbent for the removal of heavy metals from water through a simple optimal co-precipitation technique, in which the surface functional groups make the adsorbent retaining high levels of operating convenience in adsorption and desorption processes. Depending on the solution pH, the surface oxide acts as acid or base and undergoes protonation or deprotonation. Electrostatic interactions may also take place among heavy metal ions and the surface oxides [33]. High surface negative charges of FeCt also facilitate the fast migration of positive charged heavy metals to the periphery of the FeCt through electrostatic attraction. It can be concluded that both physical and chemical adsorption are greatly essential in heavy metal removal from water, which improve the absorptive capacity of FeCt for heavy metals [16,22,24,31].

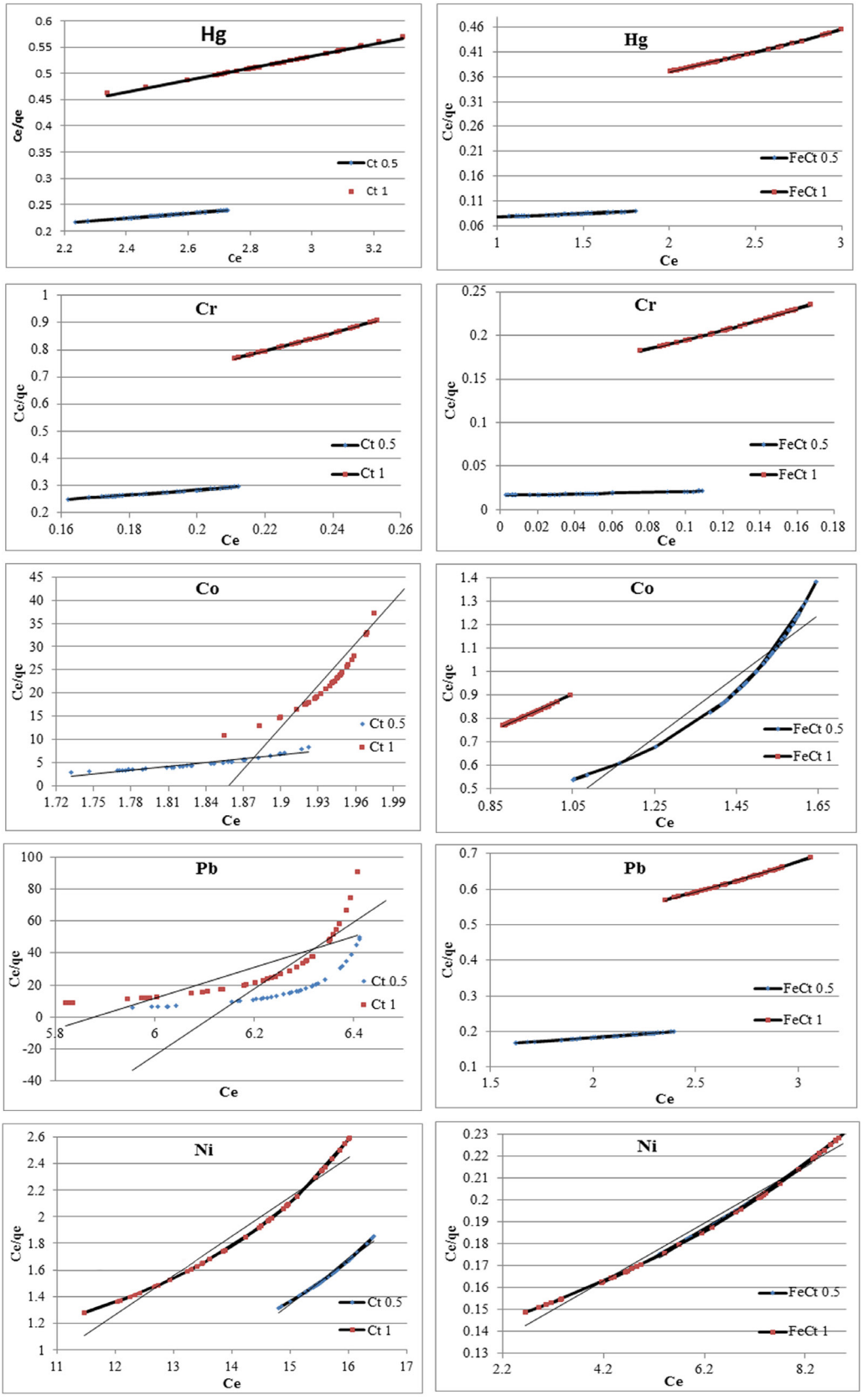

Fig. 6. Adsorption equilibrium isotherm of Hg^{2+}, Cr^{3+}, Co^{2+}, Pb^{2+}, and Ni^{2+} removal onto Ct and FeCt at the concentrations of 0.5 and 1 g. Langmuir isotherm fitting curve (equilibrium time 50 min).

Table 3
Langmuir adsorption isotherm parameters and the correlation coefficients of Hg^{2+}, Cr^{3+}, Co^{2+}, Pb^{2+}, and Ni^{2+} removal onto Ct and FeCt at the concentrations of 0.5 and 1 g

Metals	Ct 0.5 g			FeCt 0.5 g			Ct 1 g			FeCt 1 g		
	Q	*b*	R^2	*Q*	*b*	R^2	*Q*	*b*	R^2	*Q*	*b*	R^2
Hg	21.2766	0.4226	0.999	71.429	0.218	0.998	8.772	0.5977	0.99	11.807	0.4241	0.997
Cr	1.07192	9.5193	0.999	22.730	2.701	0.995	0.301	52.112	0.99	1.7431	4.1663	0.996
Co	0.03718	0.6049	0.93	0.7691	1.433	0.927	0.004	0.5381	0.69	1.3033	8.1801	0.998
Pb	0.00480	0.1635	0.16	24.155	0.414	0.997	0.011	0.1701	0.67	6.1088	0.8994	0.997
Ni	3.04414	0.0916	0.99	69.445	0.147	0.995	3.398	0.1297	0.97	75.758	0.1222	0.988

Table 4
Freundlich adsorption isotherm parameters and the correlation coefficients of Hg^{2+}, Cr^{3+}, Co^{2+}, Pb^{2+}, and Ni^{2+} removal onto Ct and FeCt at the concentrations of 0.5 and 1 g

Metals	Ct 0.5 g			FeCt 0.5 g			Ct 1 g			FeCt 1 g		
	K	*n*	R^2	*K*	*n*	R^2	*K*	*n*	R^2	*K*	*n*	R^2
Hg	15.63	1.960	0.997	12.8	4.464	0.989	8.694	1.612	0.992	7.73	2.00	0.993
Cr	0.203	1.562	0.997	0.68	14.70	0.792	0.066	1.086	0.997	0.18	3.125	0.984
Co	151.8	0.100	0.978	2.29	0.499	0.963	2.7×10^5	0.044	0.921	1.02	1.136	0.998
Pb	1.6×10^{25}	0.031	0.723	12.1	2.222	0.993	4.198	0.046	0.907	7.55	1.428	0.996
Ni	7.9×10^4	0.304	0.995	69.7	2.032	0.990	1,992.05	0.458	0.981	27.6	2.631	0.958

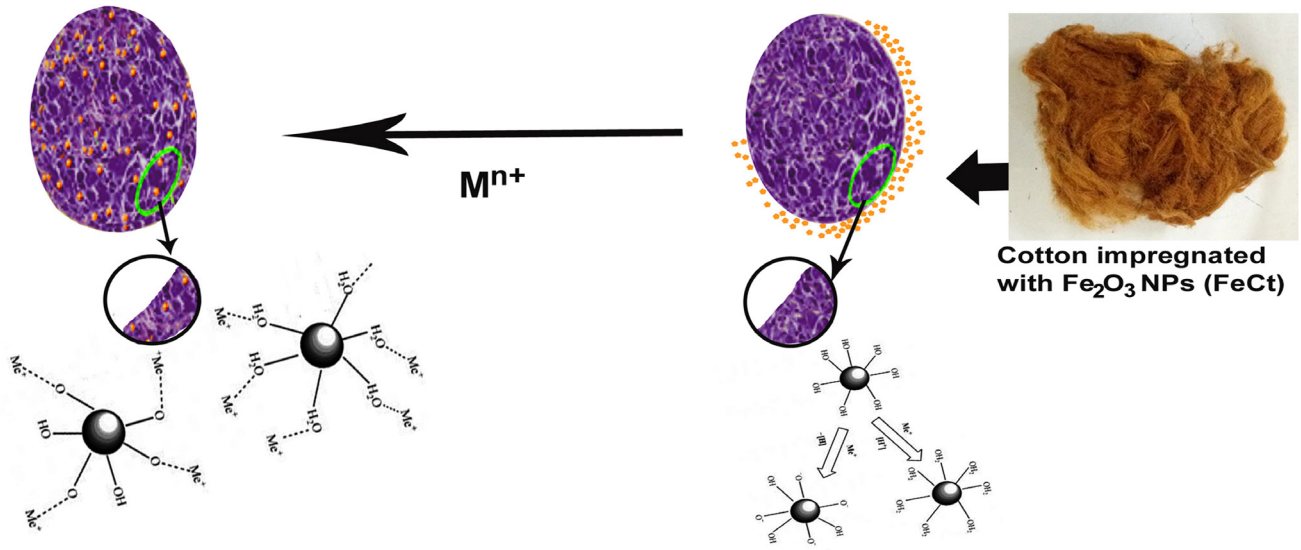

Fig. 7. Schematic depiction of the preparation of FeCt and the adsorption mechanism of heavy metal ions by FeCt.

3.7. Statistical analysis

Treatment effect on five metal elements using control (cotton/cellulose) and FeCt groups is shown in Fig. 8. Treatment of FeCt on elements Hg, Cr, and Co shows more variation as compared with other two metal elements (Pb and Ni) and for control group there is less variation as compared with the treatment group.

To prove this argument statistically, Hotelling t^2 test was used in which the null hypothesis is the equality of treatment means against the alternative that any of two treatments are not equal. *P* value of this test is less than the significance level (0.05) so we do not accept the null hypothesis and we may conclude that any of the two treatments means are not equal. Therefore, to check which treatment means are different, *t* test was used (Table 5).

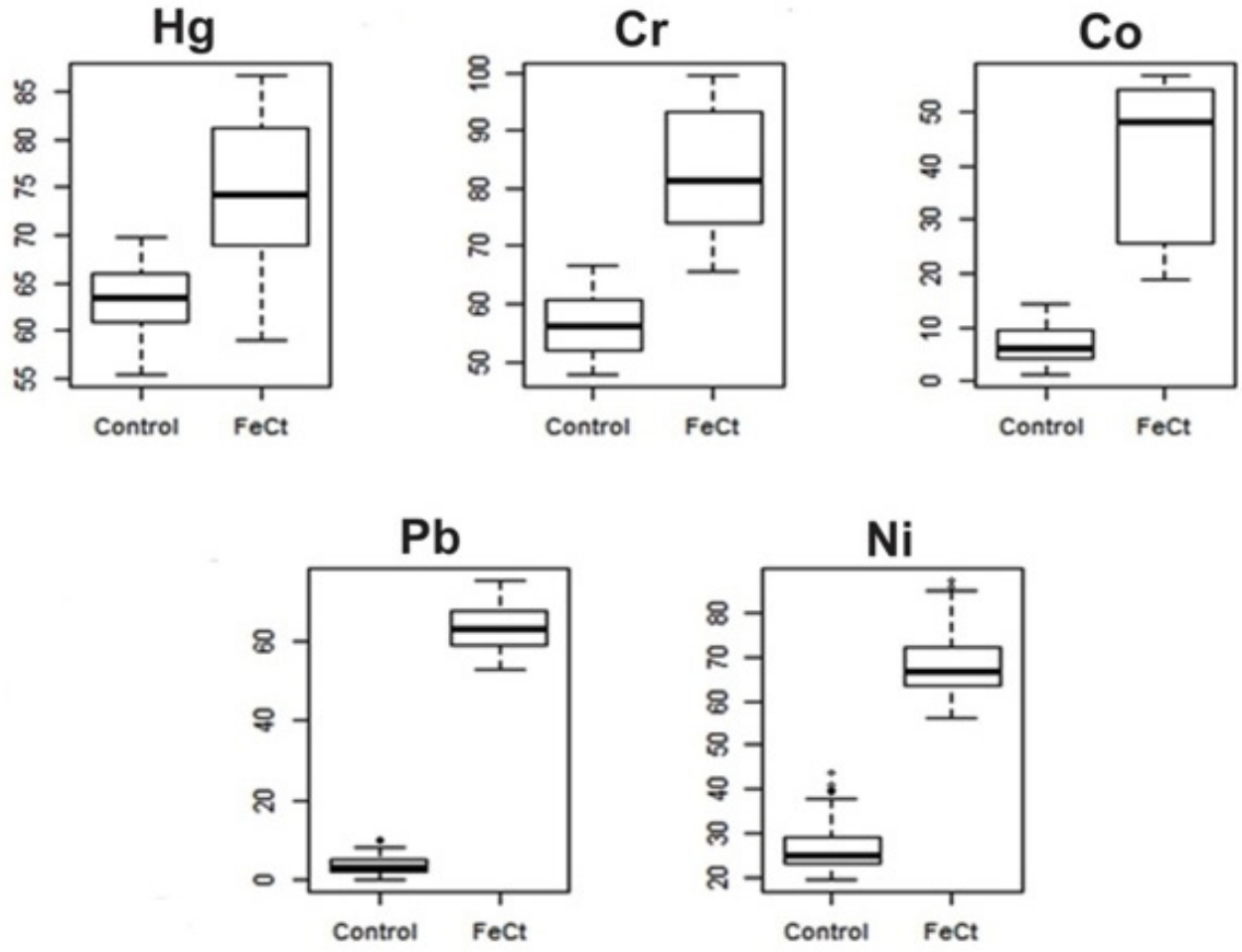

Fig. 8. Hotelling's t^2 statistic aimed at the treatment effects of control and FeCt on metal ions.

Table 5
Sample descriptive using *t* test for equality of means to compare the effects of adsorbents (FeCt) on metal ions

	Hg	Cr	Co	Pb	Ni
Mean of FeCt group	74.39614	82.82758	40.804074	63.225819	68.22273
Mean of control group	63.40477	56.39433	6.950617	3.886936	27.18377
t Statistic	–11.504	–19.938	–20.683	–90.216	–38.047
P value	2.2e–16	2.2e–16	2.2e–16	2.2e–16	2.2e–16

Concentration dependant adsorption has two levels. Fig. 9 shows there is almost the same variation for all the metals for the treatment effect except for Co metal.

P value of Hotelling t^2 test shows that all the treatment means are not equal. To check which treatment means are not equal, again *t* test was used against each metal (Table 6).

4. Conclusion

In present work, environment friendly, cotton (cellulose-based) fibers were fabricated with iron oxide NPs by simple co-precipitation method. The influence of experimental conditions over the adsorption phenomenon reveals that adsorption processes can be controlled by combining physical and chemical adsorptive mechanisms. The unique characteristics of the FeCt such as large surface area, enhanced adsorption sites in the form of porous microsphere and inherent magnetic properties makes it a promising candidate for heavy metal remediation. Batch experimental study elucidates that the adsorption process is very fast and within short contact time. The adsorbent showed high removal efficiency of Hg^{2+}, Ni^{2+}, Pb^{2+}, and Cr^{3+} species. The adsorption of all metallic ions by FeCt is

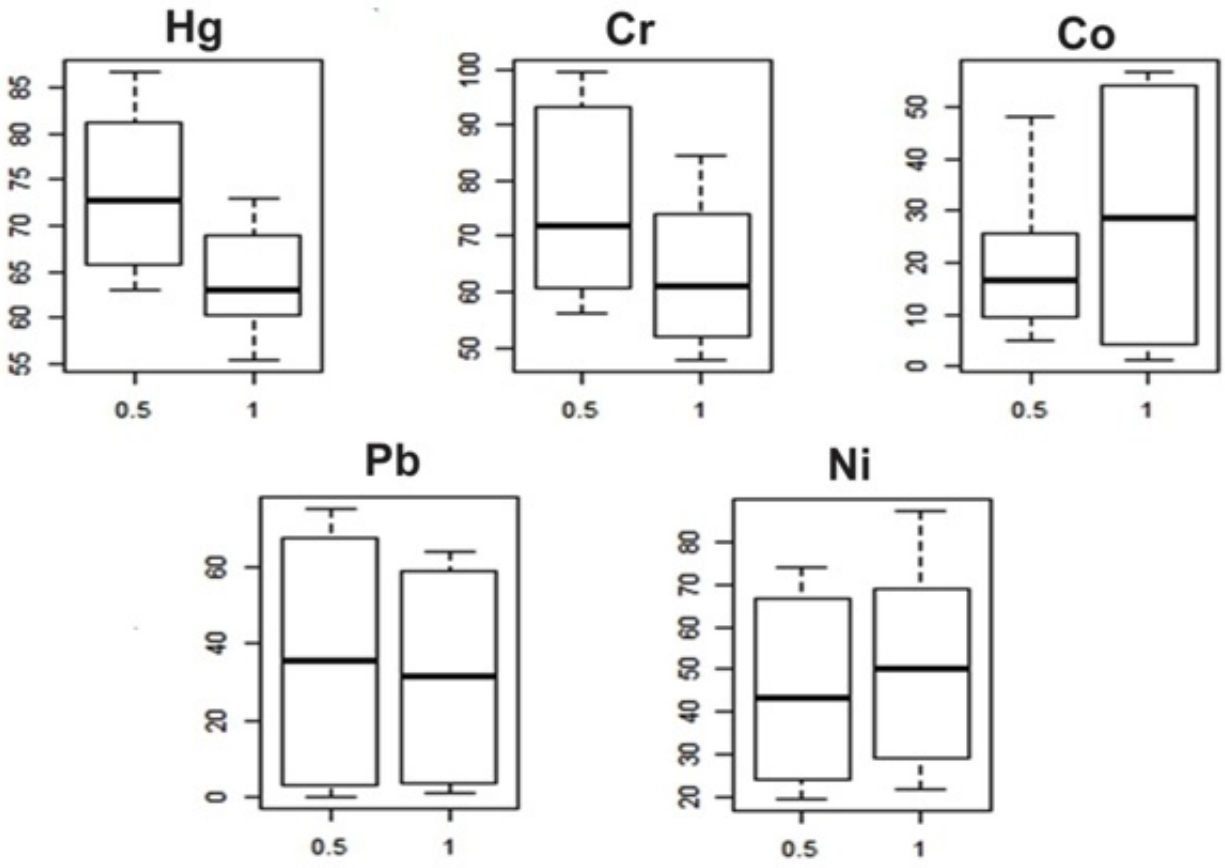

Fig. 9. Hotelling's t^2 statistics aimed at treatment effects on metal ions by different concentration levels of adsorbents (control and FeCt) at 0.5 and 1 g.

Table 6
t Test results comparing different concentrations of adsorbents for equality of means

	Hg	Cr	Co	Pb	Ni
Mean of group 0.5	73.54195	76.04407	18.65963	35.52766	45.10433
Mean of group 1	64.25896	63.17784	29.09506	31.58510	50.30216
t Statistic	8.7244	5.6794	–3.4324	0.82896	–1.5227
P value	1.23e–14	7.13e–08	0.0008466	0.4084	0.1298

predominant by electrostatic attraction between the adsorbents surface and heavy metals. The competitive capacity of all five metals onto the adsorbents follow the adsorption order as $Ni^{2+} > Hg^{2+} > Pb^{2+} > Cr^{3+} > Co^{2+}$. Fitting equilibrium data to the Langmuir and Freundlich isotherms revealed that the metals adsorption study are in good agreement with the Langmuir isotherm. The sorption process also follows pseudo-second-order rate kinetics compared with pseudo-first-order rate kinetics, as demonstrated by higher values of the correlation coefficient. Moreover, FeCt are amenable to easy filtration, forbidding draining out of the metal adsorbed grains through the filters during filtration process. These characteristics make the prepared nano-magnetic cotton cellulose promising in the field of wastewater treatment.

Acknowledgment

The authors are thankful to Higher Education Commission (HEC) Pakistan for funding for this project to Mr. Attarad Ali under Indigenous Scholarship Scheme.

Conflict of interest

The authors declare no conflict of interest.

References

[1] A. Oladipo, M. Gazi, Application of Hydroxyapatite-Based Nanoceramics in Wastewater Treatment: Synthesis, Characterization, and Optimization, A.K. Mishra, Ed., Sol-Gel Based Nanoceramic Materials: Preparation, Properties and Applications, Springer, 2017, pp. 231–251.

[2] P.A. Turhanen, J.J. Vepsäläinen, S. Peräniemi, Advanced material and approach for metal ions removal from aqueous solutions, Sci. Rep., 5 (2015).
[3] D. Nagai, A. Nakazato, H. Morinaga, Facile and efficient recovery of mercury based on poly (amine-ester)-bearing metal-complexation and acidic aqueous solution-soluble groups, Polym. J., 47 (2015) 761.
[4] M.W. Raja, Q.A. Islam, R.N. Basu, Oxygen separation membrane derived from aquatic weed: a novel bio-inspired approach to synthesize $BaBi_{0.2}Co_{0.35}Fe_{0.45}O_{3-\delta}$ perovskite from water hyacinth (*Eichhornia crassipes*), J. Membr. Sci., 522 (2017) 168–174.
[5] A. Ali, H. Zafar, M. Zia, I.U. Haq, A.R. Phull, J.S. Ali, A. Hussain, Synthesis, characterization, applications, and challenges of iron oxide nanoparticles, Nanotechnol. Sci. Appl., 9 (2016) 49.
[6] W. Wei, Q. Wang, A. Li, J. Yang, F. Ma, S. Pi, D. Wu, Biosorption of Pb (II) from aqueous solution by extracellular polymeric substances extracted from *Klebsiella* sp. J1: adsorption behavior and mechanism assessment, Sci. Rep., 6 (2016).
[7] E. Abdel-Halim, S.S. Al-Deyab, Removal of heavy metals from their aqueous solutions through adsorption onto natural polymers, Carbohydr. Polym., 84 (2011) 454–458.
[8] A.P. Lim, A.Z. Aris, A review on economically adsorbents on heavy metals removal in water and wastewater, Rev. Environ. Sci. Biotechnol., 13 (2014) 163–181
[9] M.-R. Huang, S. Li, X.-G. Li, Longan shell as novel biomacromolecular sorbent for highly selective removal of lead and mercury ions, J. Phys. Chem. B, 114 (2010) 3534–3542.
[10] A.D. Khasbaatar, Y.J. Chun, U.S. Choi, Trivalent metal adsorption properties on synthesized viscose rayon succinate, Polym. J., 40 (2008) 302–309.
[11] N.K. Goel, V. Kumar, N. Misra, L. Varshney, Cellulose based cationic adsorbent fabricated via radiation grafting process for treatment of dyes wastewater, Carbohydr. Polym., 132 (2015) 444–451.
[12] V.K. Gupta, S. Agarwal, P. Singh, D. Pathania, Acrylic acid grafted cellulosic *Luffa cylindrical* fiber for the removal of dye and metal ions, Carbohydr. Polym., 98 (2013) 1214–1221.
[13] Y. Zhao, X. Li, L. Liu, F. Chen, Fluoride removal by Fe(III)-loaded ligand exchange cotton cellulose adsorbent from drinking water, Carbohydr. Polym., 72 (2008) 144–150.
[14] Á.G. Paulino, A.J. da Cunha, R.V. da Silva Alfaya, A.A. da Silva Alfaya, Chemically modified natural cotton fiber: a low-cost biosorbent for the removal of the Cu(II), Zn(II), Cd(II), and Pb(II) from natural water, Desal. Wat. Treat., 52 (2014) 4223–4233.
[15] M. Barathi, A.S.K. Kumar, N. Rajesh, A novel ultrasonication method in the preparation of zirconium impregnated cellulose for effective fluoride adsorption, Ultrason. Sonochem., 21 (2014) 1090–1099.
[16] D. Lu, Q. Cao, X. Li, X. Cao, F. Luo, W. Shao, Kinetics and equilibrium of Cu(II) adsorption onto chemically modified orange peel cellulose biosorbents, Hydrometallurgy, 95 (2009) 145–152.
[17] X. Sun, L. Yang, Q. Li, J. Zhao, X. Li, X. Wang, H. Liu, Amino-functionalized magnetic cellulose nanocomposite as adsorbent for removal of Cr(VI): synthesis and adsorption studies, Chem. Eng. J., 241 (2014) 175–183.
[18] C. Zang, D. Zhang, J. Xiong, H. Lin, Y. Chen, Preparation of a novel adsorbent and heavy metal ion adsorption, J. Eng. Fibers Fabr., 9 (2014) 165–170.
[19] W. Teng, J. Fan, W. Wang, N. Bai, R. Liu, Y. Liu, Y. Deng, B. Kong, J. Yang, D. Zhao, W.X. Zhang, Nanoscale zero-valent iron in mesoporous carbon (nZVI@C): stable nanoparticles for metal extraction and catalysis, J. Mater. Chem. A, 5 (2017) 4478–4485.
[20] A. Ali, S. Ambreen, R. Javed, S. Tabassum, I.U. Haq, M. Zia, ZnO nanostructure fabrication in different solvents transforms physio-chemical, biological and photodegradable properties, Mater. Sci. Eng., C, 74 (2017) 137–145.
[21] T.A. Dankovich, D.G. Gray, Bactericidal paper impregnated with silver nanoparticles for point-of-use water, Environ. Sci. Technol., 45 (2011) 1992–1998.
[22] X. Luo, X. Lei, N. Cai, X. Xie, Y. Xue, F. Yu, Removal of heavy metal ions from water by magnetic cellulose-based beads with embedded chemically modified magnetite nanoparticles and activated carbon, ACS Sustain. Chem. Eng., 47 (2016) 3960–3969.
[23] J.S. Pang, A.H. Deng, L.B. Mao, X.J. Peng, J. Zhu, Adsorption of heavy metal ions by carbon-coated iron nanoparticles, Carbon, 56 (2013) 395.
[24] P. Xu, G.M. Zeng, D.L. Huang, C. Lai, M.H. Zhao, Z. Wei, G.X. Xie, Adsorption of Pb(II) by iron oxide nanoparticles immobilized *Phanerochaete chrysosporium*: equilibrium, kinetic, thermodynamic and mechanisms analysis, Chem. Eng. J., 203 (2012) 423–431.
[25] V. Madhavi, T.N.V.K.V. Prasad, A.V.B. Reddy, B.R. Reddy, G. Madhavi, Application of phytogenic zerovalent iron nanoparticles in the adsorption of hexavalent chromium, Spectrochim. Acta, Part A, 116 (2013) 17–25.
[26] J.F. Liu, Z.S. Zhao, G.B. Jiang, Coating Fe_3O_4 magnetic nanoparticles with humic acid for high efficient removal of heavy metals in water, Environ. Sci. Technol., 42 (2008) 6949–6954.
[27] X. Xin, Q. Wei, J. Yang, L. Yan, R. Feng, G. Chen, H. Li, Highly efficient removal of heavy metal ions by amine-functionalized mesoporous Fe_3O_4 nanoparticles, Chem. Eng. J., 184 (2012) 132–140.
[28] S. Rajput, L.P. Singh, C.U. Pittman, D. Mohan, Lead (Pb^{2+}) and copper (Cu^{2+}) remediation from water using superparamagnetic maghemite (γ-Fe_2O_3) nanoparticles synthesized by flame spray pyrolysis (FSP), J. Colloid Interface Sci., 492 (2017) 176–190.
[29] C.Y. Cao, J. Qu, W.S. Yan, J.F. Zhu, Z.Y. Wu, W.G. Song, Low-cost synthesis of flowerlike α-Fe_2O_3 nanostructures for heavy metal ion removal: adsorption property and mechanism, Langmuir, 28 (2012) 4573–4579.
[30] Y.C. Sharma, V. Srivastava, C.H. Weng, S.N. Upadhyay, Removal of Cr(VI) from wastewater by adsorption on iron nanoparticles, Can. J. Chem. Eng., 87 (2009) 921–929.
[31] E. Ghasemi, A. Heydari, M. Sillanpää, Superparamagnetic Fe_3O_4@EDTA nanoparticles as an efficient adsorbent for simultaneous removal of Ag(I), Hg(II), Mn(II), Zn(II), Pb(II) and Cd(II) from water and soil environmental Samples, Microchem. J., 131 (2017) 51–56.
[32] A. Ali, I.U. Haq, J. Akhtar, M. Sher, N. Ahmed, M. Zia, Synthesis of Ag-NPs impregnated cellulose composite material: its possible role in wound healing and photocatalysis, IET Nanobiotechnol., 11 (2016) 477–484.
[33] A. Ali, S. Ambreen, Q. Maqbool, S. Naz, M.F. Shams, M. Ahmad, A.R. Phull, M. Zia, Zinc impregnated cellulose nanocomposites: synthesis, characterization and applications, J. Phys. Chem. Solids, 98 (2016) 174–182.
[34] W. Jiang, H.C. Yang, S.Y. Yang, H.E. Horng, J.C. Hung, Y.C. Chen, C.Y. Hong, Preparation and properties of superparamagnetic nanoparticles with narrow size distribution and biocompatible, J. Magn. Magn. Mater., 283 (2004) 210–214.
[35] L. Bao, X. Li, Towards textile energy storage from cotton T-shirts, Adv. Mater., 24 (2012) 3246–3252.
[36] S. Mun, M. Yadav, J.-H. Kim, J. Kim, SPIE Smart Structures and Mater + Nondestructive Evaluation and Health Monitoring, 943411-943411-943415 (International Society for Optics and Photonics).
[37] S. Mitra, S. Das, K. Mandal, S. Chaudhuri, Synthesis of a α-Fe_2O_3 nanocrystal in its different morphological attributes: growth mechanism, optical and magnetic properties, Nanotechnology, 18 (2007) 275608.
[38] M. Balamurugan, S. Saravanan, T. Soga, Erratum: synthesis of iron oxide nanoparticles by using eucalyptus globulus plant extract, e-J. Surf. Sci. Nanotechnol., 12 (2014) 395.
[39] S. Sahoo, K. Agarwal, A. Singh, B. Polke, K. Raha, Characterization of γ- and α-Fe_2O_3 nano powders synthesized by emulsion precipitation-calcination route and rheological behaviour of α-Fe_2O_3, Int. J. Eng. Sci. Technol., 2 (2010) 118–126.
[40] H.C. Vu, A.D. Dwivedi, T.T. Le, S.H. Seo, E.J. Kim, Y.S. Chang, Magnetite graphene oxide encapsulated in alginate beads for enhanced adsorption of Cr(VI) and As(V) from aqueous solutions: role of crosslinking metal cations in pH control, Chem. Eng. J., 307 (2017) 220–229.

[41] E. Mekonnen, M. Yitbarek, T.R. Soreta, Kinetic and thermodynamic studies of the adsorption of Cr(VI) onto some selected local adsorbents, S. Afr. J. Chem., 68 (2015) 45–52.
[42] K.-Y. Shin, J.-Y. Hong, J. Jang, Heavy metal ion adsorption behavior in nitrogen-doped magnetic carbon nanoparticles: isotherms and kinetic study, J. Hazard. Mater., 190 (2011) 36–44.
[43] A.A. Atia, A.M. Donia, S.A. El-Enein, A.M. Yousif, Effect of chain length of aliphatic amines immobilized on a magnetic glycidyl methacrylate resin towards the uptake behavior of Hg(II) from aqueous solutions, Sep. Sci. Technol., 42 (2007) 403–420.
[44] A.R. Kul, H. Koyuncu, Adsorption of Pb(II) ions from aqueous solution by native and activated bentonite: kinetic, equilibrium and thermodynamic study, J. Hazard. Mater., 179 (2010) 332–339.
[45] S.K. Singh, T.G. Townsend, D. Mazyck, T.H. Boyer, Equilibrium and intra-particle diffusion of stabilized landfill leachate onto micro- and meso-porous activated carbon, Water Res., 46 (2012) 491–499.
[46] A.A. Atia, A.M. Donia, A.E. Shahin, Studies on the uptake behavior of a magnetic Co_3O_4-containing resin for Ni(II), Cu(II) and Hg(II) from their aqueous solutions, Sep. Purif. Technol., 46 (2005) 208–213.
[47] N.S.A.A. Hamid, N.A.C. Malek, H. Mokhtar, W.S. Mazlan, R.M. Tajuddin, Removal of oil and grease from wastewater using natural adsorbents, J. Teknologi, 78 (2016) 97–102.